International Journal of Power Electronics and Drive System (IJPEDS)
Vol. 17, No. 3, September 2026, pp. 2197~2209
ISSN: 2088-8694, DOI: 10.11591/ijpeds.v17.i3.pp2197-2209

Real time fuzzy energy management of hybrid storage systems in DC microgrids with dynamic voltage restorer assisted power quality enhancement

Yacine Benatallah[1], Abdelkrim Benali[1], Mabrouk Dahane[1], Somia Benali[2]
[1]ILAM Laboratory, Department of Electrical Engineering, Institute of Technology, Nour Bachir El-Bayadh University Center, El Bayadh, Algeria
[2]Department of Commercial Sciences, Faculty of Economic, Commercial and Management Sciences, Ahmed Zabana Relizane University, Relizane, Algeria

Article Info

Article history:

Received Apr 20, 2026
Revised Aug 21, 2026
Accepted Aug 24, 2026

Keywords:

DVR
Fuel cell
Fuzzy EMS
Hybrid DC microgrid
Power quality DC bus
Regulation
Voltage sag/swell
compensation

ABSTRACT

This paper presents a real-time fuzzy logic–based energy management system (EMS) for a hybrid DC microgrid supplying a constant DC load and an AC sensitive load protected by a dynamic voltage restorer (DVR). The system integrates a 25-kW photovoltaic (PV) array, a 10-kW fuel cell (FC), a 15-kW battery energy storage system, and a 396 V supercapacitor bank. The EMS calculates the net power balance ($\Delta P = P_{PV} - P_{load}$), compares it with the states-of-charge (SoC) of the battery and supercapacitor, and dynamically allocates power references to each source. Fuzzy rules prioritize renewable generation, exploit the supercapacitor for fast transient compensation, and schedule the battery and fuel cell for medium- and long-term power balancing. The DVR acts as a series active power filter, injecting real power during sags and absorbing excess energy during swells, while the EMS maintains DC bus stability under fault conditions. Simulation results demonstrate enhanced DC bus voltage regulation, reduced battery cycling, efficient hydrogen utilization, and rapid recovery from voltage disturbances. The proposed strategy improves power quality and ensures continuous operation of sensitive loads, making it suitable for smart grid and renewable-based microgrid applications.

Corresponding Author:

Abdelkrim Benali
ILAM Laboratory, Department of Electrical Engineering, Institute of Technology
Nour Bachir El-Bayadh University Center
Aflou Road, BP 32000, El Bayadh, Algeria
Email: benaliabd@gmail.com

1. INTRODUCTION

The growing integration of renewable energy sources in DC microgrids supplying sensitive loads introduces significant variability in both generation and demand, resulting in voltage fluctuations and power imbalances that conventional control strategies cannot effectively handle. To overcome these challenges, energy storage systems coordinated by advanced energy management systems (EMS) are widely employed to smooth renewable intermittency, regulate the DC bus voltage, and ensure reliable power supply [1], [2]. In particular, hybrid energy storage systems combining batteries and supercapacitors enhance system resilience by improving power quality and alleviating battery stress when managed through optimized EMS strategies [3]. Nevertheless, fluctuations in renewable output, rapid load variations, and network disturbances can still lead to voltage instability and accelerated battery degradation if not properly addressed [4]-[6]. As a result, recent research has focused on integrating real-time EMS with hybrid storage and fast-response compensation techniques, including fuzzy logic control, model predictive control, and dynamic voltage restorer (DVR)-based approaches, to enhance voltage stability, optimize power sharing, and extend battery lifetime under dynamic conditions [7]-[9]. Recent contributions further advance the coordination of hybrid energy storage systems (HESS) in DC microgrids operating under intermittent renewable generation. For instance, frequency decomposition–based power-sharing strategies have been shown to improve system stability while reducing battery stress, whereas battery-supercapacitor configurations effectively mitigate DC-link voltage fluctuations under varying load and irradiance conditions [8], [9]. Moreover, model predictive control schemes have been successfully applied to handle voltage sag and swell events as well as reverse power flow in specific applications [10], while simulation results consistently demonstrate the superior transient performance of HESS compared to battery-only solutions [11].

However, most existing approaches do not integrate real-time DVR operation with fuzzy logic–based energy management while jointly considering battery and supercapacitor SoC constraints during dynamic voltage disturbances. This limitation reveals an important gap between power quality enhancement and hybrid energy management in DC microgrids. To address this issue, this paper proposes a real-time fuzzy EMS for a hybrid DC microgrid integrating a 25 kW PV array, a 10-kW fuel cell, a 15-kW battery, and a supercapacitor bank.

The proposed EMS simultaneously considers the net power balance and the state-of-charge (SoC) conditions of the battery and supercapacitor to achieve coordinated power sharing among the hybrid sources. The supercapacitor provides rapid compensation for short-term power fluctuations, while the battery and fuel cell support medium- and long-term energy requirements. In addition, a dynamic voltage restorer (DVR) is integrated to mitigate voltage sag and swell events and protect sensitive loads against voltage disturbances. Unlike conventional studies that separately investigate fuzzy EMS or DVR compensation, the proposed framework combines real-time energy management and DVR-assisted power-quality enhancement within a unified hybrid DC microgrid architecture. This coordinated strategy improves DC-link voltage stability, reduces battery stress through fast supercapacitor compensation, and enhances overall system robustness under transient operating conditions. The proposed integration therefore provides a comprehensive solution for hybrid DC microgrids requiring both efficient energy management and reliable power-quality support.

The proposed system is modelled and validated in MATLAB/Simulink under severe disturbances, including 0.2 pu voltage sag and 1.6 pu swell conditions. Simulation results demonstrate stable 500 V DC-bus regulation with voltage deviations limited to ±1.18%, together with effective coordinated power sharing among the PV, battery, fuel cell, and supercapacitor. The rapid DVR response further confirms the effectiveness of the proposed EMS–DVR framework for simultaneous energy management and power quality enhancement.

The main contributions of this work are summarized as follows: i) Development of a fuzzy EMS for dynamic power allocation among PV, fuel cell, battery, and supercapacitor based on load demand and SoC constraints; ii) Real-time integration of DVR operation with hybrid energy management for mitigation of voltage sag and swell disturbances; and iii) Validation of the proposed framework under diverse operating scenarios, demonstrating improved DC-bus stability, reduced battery cycling stress, and enhanced microgrid reliability compared with conventional EMS approaches.

The remainder of the paper is organized as follows: i) Section 2 presents the hybrid DC microgrid architecture, hybrid storage configuration, fuzzy-based EMS, and DVR-assisted control model; ii) Section 3 discusses the simulation setup, operating scenarios, and system performance under normal and disturbed conditions, including comparative analysis and practical considerations; and iii) Finally, Section 4 concludes the paper and outlines future research directions.

2. METHOD

Figure 1 illustrates the proposed hybrid energy storage DC microgrid, which supplies constant DC loads and sensitive AC loads through a dynamic voltage restorer (DVR) for mitigating voltage sags, swells, and transient disturbances. The system integrates multiple distributed energy resources (DERs) with dedicated power electronic converters to achieve coordinated energy management and enhanced power quality. The PV array provides the primary renewable source with a rated power of 25 kW, while the 10-kW fuel cell acts as an auxiliary and dispatchable source during energy deficits. A 15-kW battery, modelled using a Thevenin equivalent, provides medium- and long-term energy balancing, whereas the supercapacitor bank supplies high-power, short-duration buffering to compensate for rapid load variations and voltage transients. The PV array is connected to the DC bus through a unidirectional DC/DC boost converter equipped with MPPT to maximize energy extraction under variable irradiance. In contrast, the battery and supercapacitor are interfaced through bidirectional DC/DC converters, enabling controlled charging and discharging while supporting DC-bus voltage stabilization. The fuel cell is connected through a DC/DC converter to regulate its output and provide dispatchable power when renewable generation and storage are insufficient. This configuration enables coordinated operation of the energy sources and storage units while allowing the DVR to provide rapid voltage compensation for sensitive loads.

A fuzzy logic–based EMS coordinates the operation of the PV array, battery, supercapacitor, and fuel cell according to load demand, power balance, and storage SoC conditions. The supercapacitor provides fast compensation for short-term power fluctuations, while the battery and fuel cell support medium- and long-term energy requirements, thereby improving renewable energy utilization and reducing battery stress. In parallel, the DVR provides rapid compensation during voltage sag and swell events, supporting stable operation of sensitive loads. The coordinated EMS–DVR strategy therefore enables simultaneous energy management, DC-bus stabilization, and power-quality enhancement under varying operating conditions [12], [13].

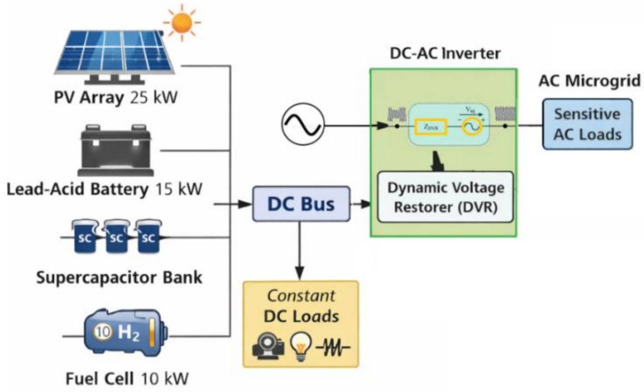

Figure 1. System overview

2.1. PV model

The photovoltaic (PV) array is the primary 25 kW energy source operating on a 500 V DC bus and is modelled using a single-diode equivalent to capture irradiance- and temperature-dependent I–V behaviour [14], [15]. The output current is given by (1), incorporating photocurrent I_{ph}, diode saturation current I_s, series R_s and R_{sh} shunt resistances, and thermal effects V_T. For efficient energy extraction, the PV array is interfaced through a unidirectional DC–DC boost converter controlled by a perturb-and-observe MPPT algorithm, which regulates operation at the maximum power point under varying irradiance conditions [16].

$$I = I_{ph} - I_s\left(e^{\frac{V_{PV}+I_{PV}.R_S}{\eta V_T}} - 1\right) - \frac{V_{PV}+I_{PV}R_S}{R_{sh}} \quad (1)$$

2.2. FC model

The proton exchange membrane fuel cell (PEMFC) is modelled as a dynamic system in which variations in reactant partial pressures, operating temperature, and gas flow rates influence the open-circuit voltage E_{oc}, exchange current i_0, and Tafel slope A. These parameters are updated in real time to accurately represent activation, ohmic, and concentration losses within the fuel cell stack. The open-circuit voltage is calculated using the Nernst (2): with $A=RT/(z\alpha F)$ and $i_0=i_{0,reff}(T, P_{H2}, P_{O2})$. Here, R is the gas constant, F the Faraday constant, and α the charge transfer coefficient; P_{H2} and P_{O2} denote the partial pressures of hydrogen and oxygen. This model captures temperature- and pressure-dependent PEMFC effects, with real-time updates of E_{oc}, i_0, and A enabling accurate dynamic and steady-state modelling of PEMFC behaviour under varying temperature, pressure, and load conditions, enabling realistic prediction of polarization losses and transient response for hybrid microgrid studies [17]-[19].

$$E_{oc} = K_c + E_n = \frac{zFk(P_{H2}+P_{O2})^{\Delta v}}{Rh} e^{-\frac{\Delta G}{RT}} \quad (2)$$

2.3. Acid lead battery model

The lead–acid battery is modelled as a SOC-dependent controlled voltage source governed by the Shepherd (3) [20], where E_0 is the open-circuit voltage, K the polarization constant, $Rint$ the internal resistance, A and B exponential parameters, and $vp(t)$ the transient voltage component.

$$v_b(t) = E_0 - K\frac{Q}{Q-it(t)}\, i(t) - R_{int}\, i(t) + A\, e^{-B\, it(t)} + v_p(t) \quad (3)$$

The state of charge is computed as (4), where $Qnom$ is the nominal capacity and $\eta(i)$ is the Coulombic efficiency (ηch = 0.85-0.95, $\eta dis \approx 1$). The semi-empirical model accurately captures lead-acid battery nonlinearities, high-current voltage drops, exponential behaviour near full charge, and low SoC voltage decay with parameters identified from manufacturer data or experimental tests [21].

$$SoC(t) = SoC(0) - \frac{1}{Q_{nom}} \int_0^t \eta(i)\, i(\tau)\, d\tau \quad (4)$$

2.4. Supercapacitor (SC) model

Supercapacitors offer fast, high-power transient support in the DC microgrid, mitigating voltage fluctuations and relieving battery stress, and are modelled using a simple ESR–C representation [22].

$$v_{sc}(t) = v_{sc}(0) + \frac{1}{C}\int_0^t i_{sc}(\tau) d\tau - i_{sc}(t) R_{ESR} \quad (5)$$

Where *C* is the capacitance, R_{ESR} the equivalent series resistance, and i_{SC} the capacitor current [23]. To capture charge redistribution and diffusion effects, a multi-RC branch model is employed:

$$v_{sc}(t) = v_C(t) - \sum_{k=1}^{n} v_{p,k}(t) \quad (6)$$

which effectively reproduces transient behaviour while remaining computationally efficient [23]. The usable energy between voltage limits V_{min} and V_{max} is $E=1/2C(V^2_{max}-V^2_{min})$, and the peak power is limited by $Peak \approx V^2/R_{ESR}$ [22]. Temperature and self-discharge effects are included through simple resistance-capacitance adjustments [24].

2.5. Energy management strategy

The proposed fuzzy logic–based EMS coordinates the hybrid DC microgrid, managing PV, battery, supercapacitor, and PEMFC operation to maintain DC bus stability, ensure reliable load supply, regulate storage SOC, and minimize fuel cell use when renewable generation is sufficient. Figure 2(a)-2(d) illustrates the proposed fuzzy input–output membership functions defining the linguistic variables for the EMS.

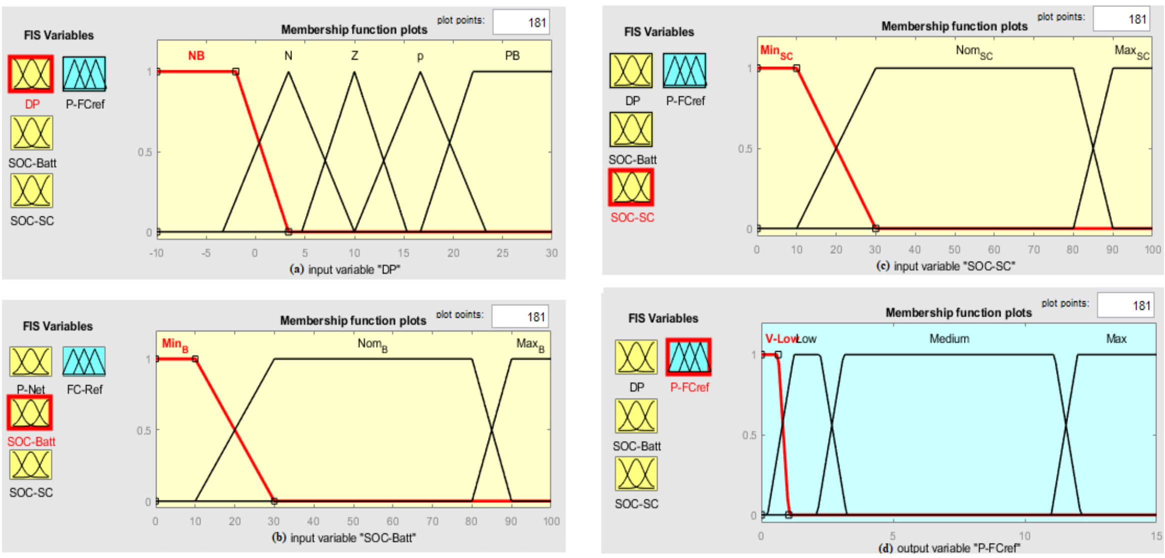

Figure 2. Fuzzy membership function plots of input variables: (a) DP, (b) SOC-batt, (c) SOC-SC, and (d) P-FCref

2.5.1. Input variables

The fuzzy EMS uses five inputs: i) DC load demand P_{load} (kW); ii) PV output P_{PV} (25 kW, 500 V); iii) Battery SoC_{Batt} (0–100%, 15 kW, 500 V); iv) Supercapacitor SoC_{SC} (0–100%, 7 kW, 500 V, 29 F); and v) Fuel cell voltage VFC (10 kW nominal, 15 kW max, 500 V), indicating FC availability.

2.5.2. Fuzzy rule-based energy management system (EMS)

A fuzzy rule-based EMS coordinates power among PV, SC, battery, and FC to meet load demand while keeping storage SoC within limits. Power deviation directs energy flow:

$$DP = P_{PV} - P_{Load} \quad (7)$$

When DP > 0, surplus PV power is used to charge the supercapacitor if SoC_{SC} is below its upper limit; otherwise, the battery is charged. When DP < 0, the supercapacitor supplies power if SOC_{SC} is above its minimum threshold; otherwise, the battery is discharged. The fuel cell is activated only when the battery SOC becomes low. The EMS follows the priority order: PV → SC → Battery → Fuel Cell. The fuzzy controller inputs are DP, SoC_{SC}, and SoC_{Batt}, while the output is the reference fuel cell power P_{FCref}. System ratings are: P_{PV} = 25 kW, battery nominal power P_{Batt} = 15 kW with SoC limits of 30–85%, supercapacitor nominal power P_{SC} = 7 kW with SoC limits of 30–85%, and fuel cell nominal-maximum powers of 10 kW and 15 kW, respectively. The fuel cell reference current is given by $I_{FCref} = P_{FCref}/V_{FC}$ with current limits of 0–50 A.

2.6. DVR control strategy

The dynamic voltage restorer (DVR) is a series-connected custom power device designed to mitigate voltage disturbances in distribution systems. By injecting a controlled voltage in series with the supply line, the DVR compensates for sags by supplying the missing voltage and for swells by absorbing the excess, thus maintaining the load voltage close to nominal. Modern DVR designs employ advanced control strategies and energy storage units to ensure fast dynamic response and minimal distortion in sensitive loads [25]. The series injected voltage of the DVR can be written as (8).

$$V_{inj} = V_L - V_S + Z_{DVR} I_L \tag{8}$$

In the integrated DVR system, the EMS regulates the DC-link voltage by coordinating the charging and discharging of the battery and supercapacitor, ensuring sufficient energy availability for DVR compensation during voltage sag and swell events. The supercapacitor provides rapid transient support, while the battery contributes to longer-duration energy balancing, thereby reducing excessive battery stress and helping maintain the storage units within their operating limits. The DVR transformer parameters, summarized in Table 1, were selected according to practical ranges commonly reported in the DVR literature, ensuring realistic voltage-injection behavior and transient compensation capability. This coordinated operation contributes to stable DC-link regulation, reliable voltage compensation, and improved overall system stability [26], [27].

Table 1. DVR transformer parameters used in the MATLAB/Simulink model and comparison with representative values reported in DVR literature

Parameter	Simulink model	Typical DVR literature range
Nominal power	4 kVA	4–10 kVA
Frequency	50 Hz	50 Hz
Primary voltage	380 V	380–415 V
Secondary voltage	380 V	380–415 V
Winding resistance	0.02 pu	0.005–0.03 pu
Leakage inductance	0.02 pu	0.01–0.04 pu

3. SIMULATION AND RESULTS

3.1. Simulation setup and scenarios

The proposed hybrid energy system integrates PV, SC, battery, and FC under a fuzzy EMS following the priority sequence PV → SC → Battery → FC. The DC bus supplies the DC load and, through the DVR, interfaces with the AC microgrid to provide voltage support and enhance power quality during disturbances. Figure 3 presents the solar irradiance profile used in the simulations, which is dynamically varied to represent changing operating conditions while maintaining a constant ambient temperature of 25 °C.

The simulation campaign evaluates system behavior under a series of scenarios:

i) Irradiance variation: The study evaluates system performance under stepped irradiance changes, allowing assessment of PV output, transient response, and EMS control effectiveness.
ii) DC load variation: The DC load is varied between 7, 15, 19, and 21 kW to evaluate power sharing among the PV, SC, battery, and FC.
iii) State-of-charge monitoring: SoC trajectories of the SC and battery are monitored to verify that the EMS maintains operation within SoC limits.
iv) Fuel cell metrics: Fuel cell current, hydrogen consumption, and efficiency are evaluated across varying load conditions.
v) DC bus voltage: DC bus voltage is monitored to ensure stability under varying source and load conditions.
vi) DVR behavior: The DVR's absorbed and injected power (P_{DVR}) and its impact on the AC microgrid voltage (supplied by the AC generator) are analyzed. All tests are initially performed under normal (non-faulted) conditions. A subsequent fault scenario includes voltage sag (0.2 pu) and a swell (1.6 pu) from 0.4–1.7 s to evaluate DVR compensation, EMS resilience, and system fault response.

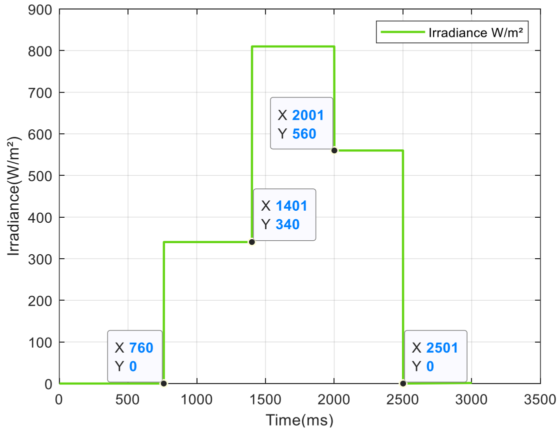

Figure 3. Irradiance profile during simulation (W/m²)

3.2. Power flow profiles under no fault

This subsection presents the power behavior of the hybrid system under the fuzzy-based EMS. It illustrates how the energy sources coordinate to meet the load following the priority sequence PV → SC → battery → FC. By examining the individual power profiles, the EMS effectiveness in maintaining energy balance, ensuring smooth transitions, and supporting DC bus voltage stability under varying irradiance and load conditions is evaluated.

Figure 4 shows power profiles of the PV array (P_{PV}), fuel cell (P_{FC}), supercapacitor (P_{SC}), Pbattery ($P_{Battery}$), and load (P_{Load}) under load levels of 7, 15, 19, and 21 kW. To evaluate the dynamic response of the proposed EMS, the solar irradiance is varied stepwise from 0 to 340, 810, 560, and 0 W/m² at t=0t=0, 0.76, 1.4, 2, and 2.5 s, respectively, reproducing rapidly changing operating conditions. Figures 4(a)–4(d) present the corresponding power-sharing responses for the four load levels, showing the coordinated operation of the hybrid sources under varying irradiance and load demand. The PV array supplies the available renewable power, while the supercapacitor rapidly compensates for short-term power imbalances; the battery and fuel cell provide additional support when required. As the load increases, the EMS dynamically adjusts the contributions of the storage units and fuel cell to maintain power balance and stable DC-bus operation.

At low irradiance levels, the fuzzy-based EMS prioritizes energy support from the supercapacitor and battery, while the fuel cell is dispatched only when the combined PV and storage power is insufficient to meet the load demand. As irradiance increases, the PV contribution rises accordingly, reducing reliance on the battery and fuel cell, and excess power is absorbed by the storage units.

3.3. Fault scenarios and DVR performance

This subsection assesses the dynamic performance of a hybrid PV–SC–Battery–FC system combined with a DVR under grid disturbances, focusing on the DVR's ability to maintain AC load voltage quality while the EMS coordinates energy delivery from the hybrid sources and stabilizes the DC link. Two fault scenarios are tested between t = 0.4 s and t = 1.7 s: a 0.2 pu voltage sag (Scenario 1) and a 1.6 pu voltage swell (Scenario 2). The DC load is fixed at 15 kW, high enough that PV alone cannot meet demand, requiring the EMS to actively coordinate the supercapacitor, battery, and fuel cell, while remaining low enough to avoid unrealistic system collapse. During each disturbance, the DVR injects compensating voltage to keep the load voltage within limits, drawing dynamic support from the hybrid sources via EMS regulation of the DC-link voltage: the supercapacitor handles fast transients, while the battery and fuel cell cover sustained loads. The evaluation examines DVR injected power, DC-link voltage stability, and AC load voltage profiles across both scenarios.

3.3.1. Case A: medium voltage sag of 0.2 pu occurring between 0.4 s and 1.7 s

Figure 5 illustrates the DVR performance during a voltage sag event. Figure 5(a) shows the onset of the sag at around 400 ms, where the supply voltage drops sharply to about 55 V, while the DVR injects a compensating voltage of approximately 221 V, maintaining the load voltage near its nominal level. Figure 5(b) represents the end of the same sag event at around 1700 ms, where the DVR continues to provide compensation until the supply voltage recovers. The results confirm the DVR’s ability to dynamically restore the load voltage throughout the entire sag period.

During the voltage sag disturbance, the total generated power and the battery contribution were analyzed over the 1300 ms interval from 400 ms to 1700 ms. The total power output from the hybrid sources-including the battery and fuel cell- is indicated by the yellow-shaded area (Area 1), situated between the cyan curve (total power under normal operation at 15 kW, no fault) and the dark blue curve (total power at 15 kW during the sag event). The battery power response is highlighted in Areas 2, 3, and 4, bounded by the yellow curve representing battery power under normal conditions and the purple curve corresponding to the sag condition. During the voltage sag, the battery increases its power contribution to compensate for the resulting power deficit and support the DC-side power balance. This coordinated response helps maintain a stable total output despite the voltage disturbance, demonstrating the battery's role in supporting system stability during transient conditions.

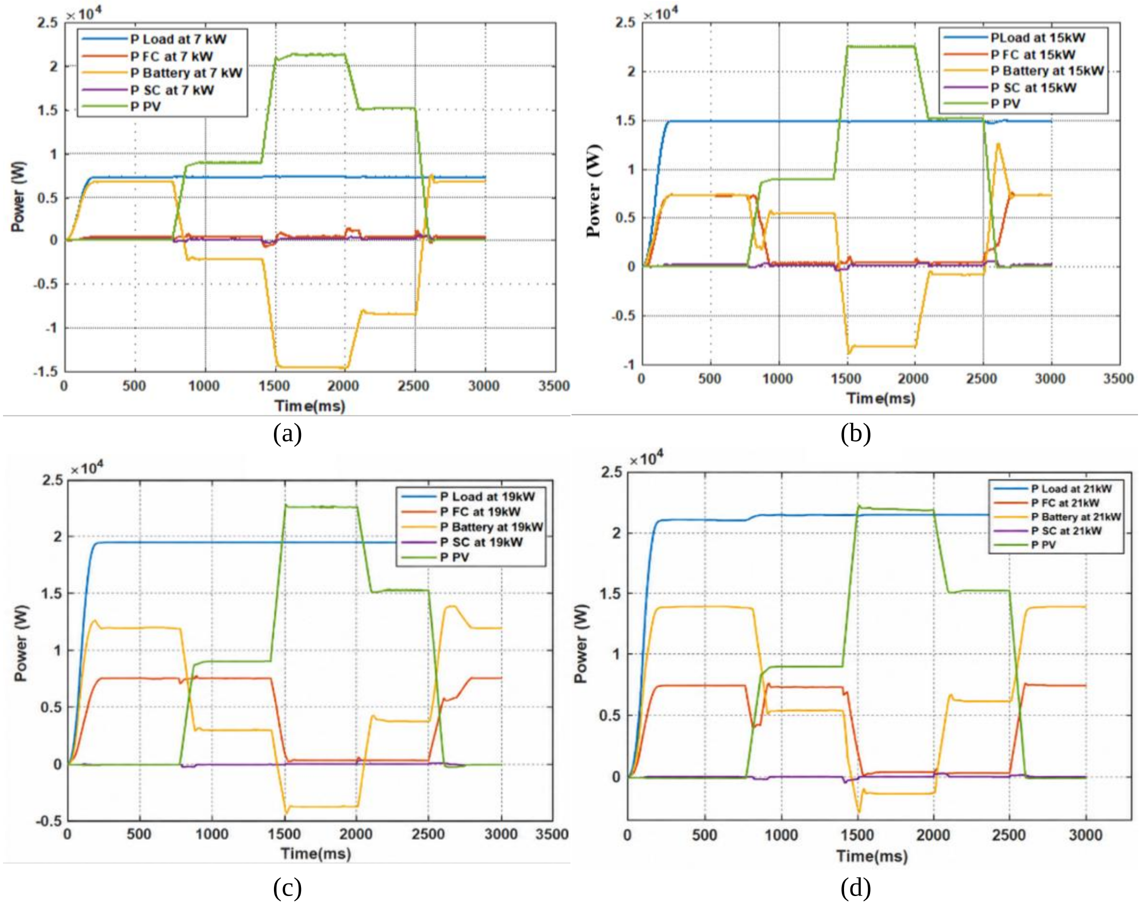

Figure 4. Power profiles of the PV array (P_{PV}), fuel cell (P_{FC}), supercapacitor (P_{SC}), Pbattery ($P_{Battery}$), and load (P_{Load}) under different DC load conditions: (a) 7 kW, (b) 15 kW, (c) 19 kW, and (d) 21 kW

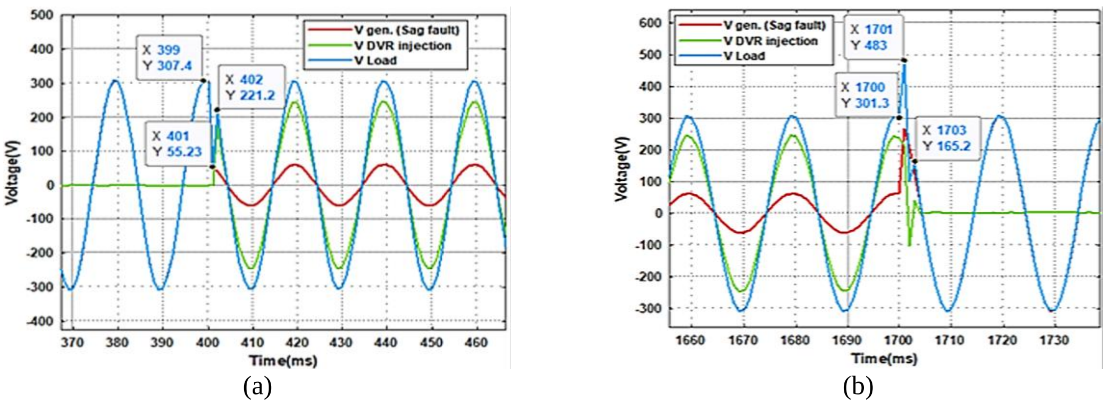

Figure 5. Single-phase voltage waveforms under a sag disturbance, illustrating (a) the instant of sag initiation and (b) voltage recovery following sag clearance

Figure 6(a) shows the battery power variation, while Figure 6(b) depicts the fuel cell power contribution during the sag disturbance (Area 5). Both plots clearly illustrate the coordinated response of the hybrid energy storage and generation units in sustaining total system power throughout the event. Figure 6(c) illustrates the supercapacitor (SC) contribution during the voltage sag disturbance.

The yellow-shaded area represents the SC active-power response during the voltage sag. The SC rapidly increases its power contribution to compensate for the transient power deficit and support the DC bus. This fast response reduces the burden on the battery and contributes to improved transient stability of the hybrid microgrid.

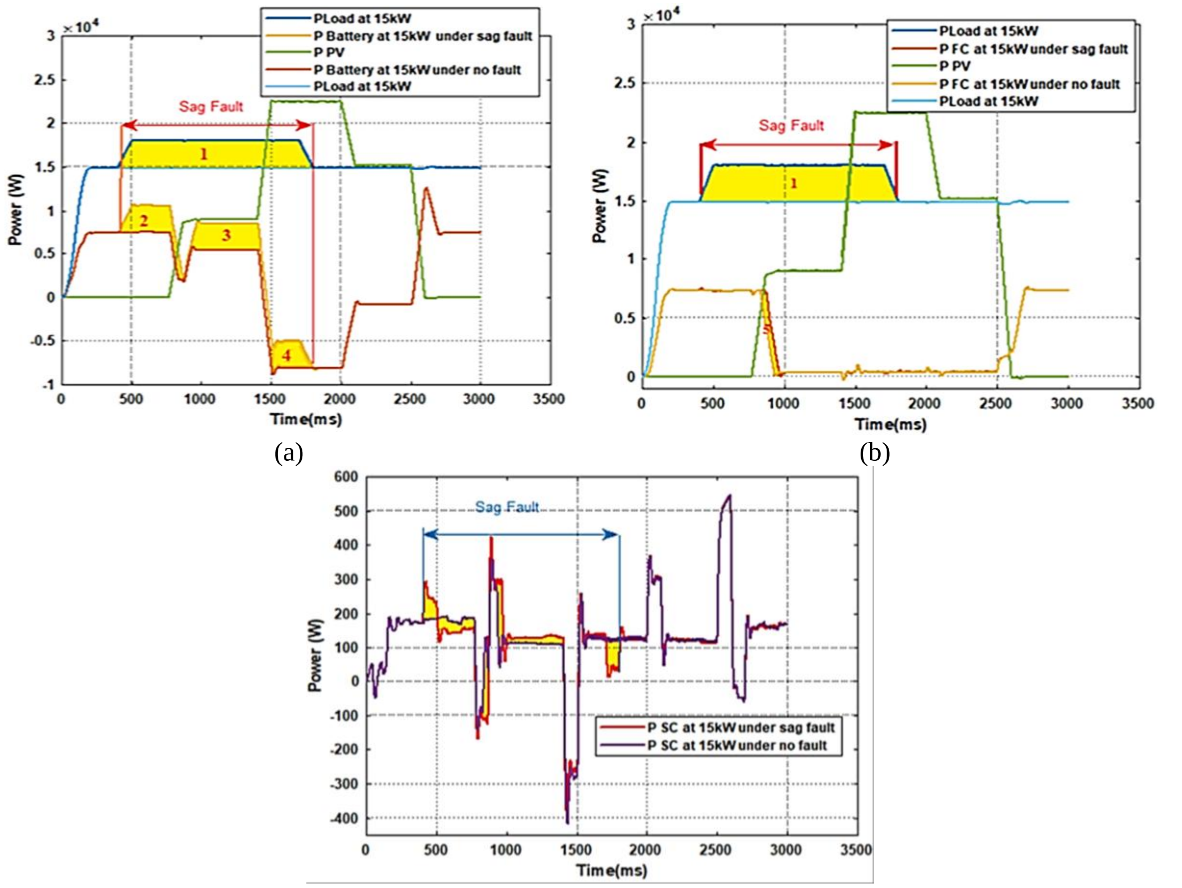

Figure 6. Contribution of battery, FC, and SC during sag disturbance: (a) battery power, (b) FC power, and (c) SC power

3.3.2. Case B: medium voltage swell of 1.6 pu occurring between 0.4 s and 1.7 s

Figure 7 shows the single-phase voltage waveforms during a voltage swell disturbance, including the supply, DVR-injected, and load voltages. In Figure 7(a), the swell begins around 400 ms, causing the supply voltage to exceed its nominal value and creating an overvoltage condition. The DVR promptly injects a compensating voltage opposite to the swell, keeping the load voltage close to its rated level. Figure 7(b) depicts the end of the swell at approximately 1.7 s, where the DVR continues to provide compensation until the disturbance clears. These results demonstrate the DVR's effectiveness in mitigating voltage swell events and maintaining stable, acceptable voltage at the load.

Figure 8 illustrates the contribution of the battery and fuel cell (FC) during a voltage swell disturbance, highlighting the coordinated power response of both sources. Figure 8 illustrates the coordinated power contributions of the battery, fuel cell (FC), and supercapacitor (SC) during a voltage swell. As shown in Figure 8(a), when PV generation temporarily exceeds the nominal 15 kW load during the swell, the battery shifts to charging mode (negative power regions), absorbing excess energy and preventing overgeneration. Simultaneously, Figure 8(b) shows that the FC output is reduced, further supporting power balance. Figure 8(c) highlights the SC's fast dynamic response during the voltage swell. The brief negative power peak indicates rapid charging, allowing the SC to absorb transient excess energy generated during the disturbance. This fast energy absorption, together with the coordinated responses of the battery and FC, helps maintain power balance, limit overvoltage effects, and enhance the transient stability of the hybrid microgrid.

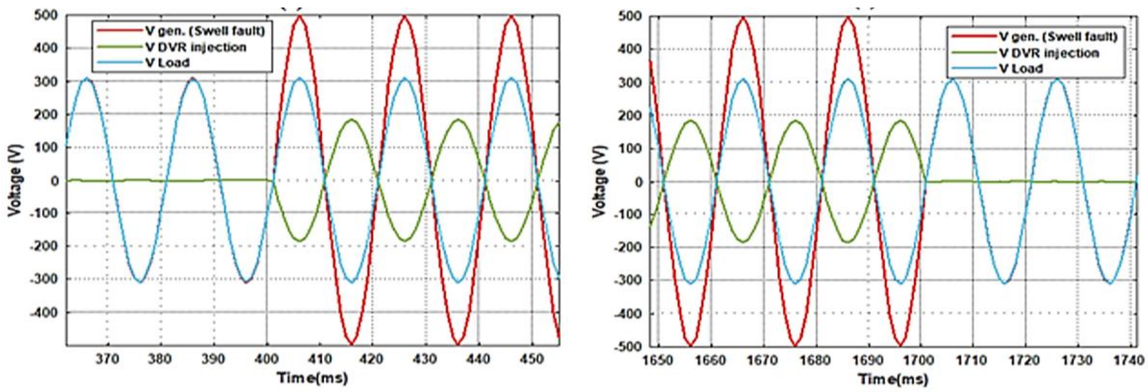

(a) (b)

Figure 7. Single-phase voltage waveforms under a swell disturbance, illustrating: (a) the instant of swell initiation and (b) voltage recovery following swell clearance

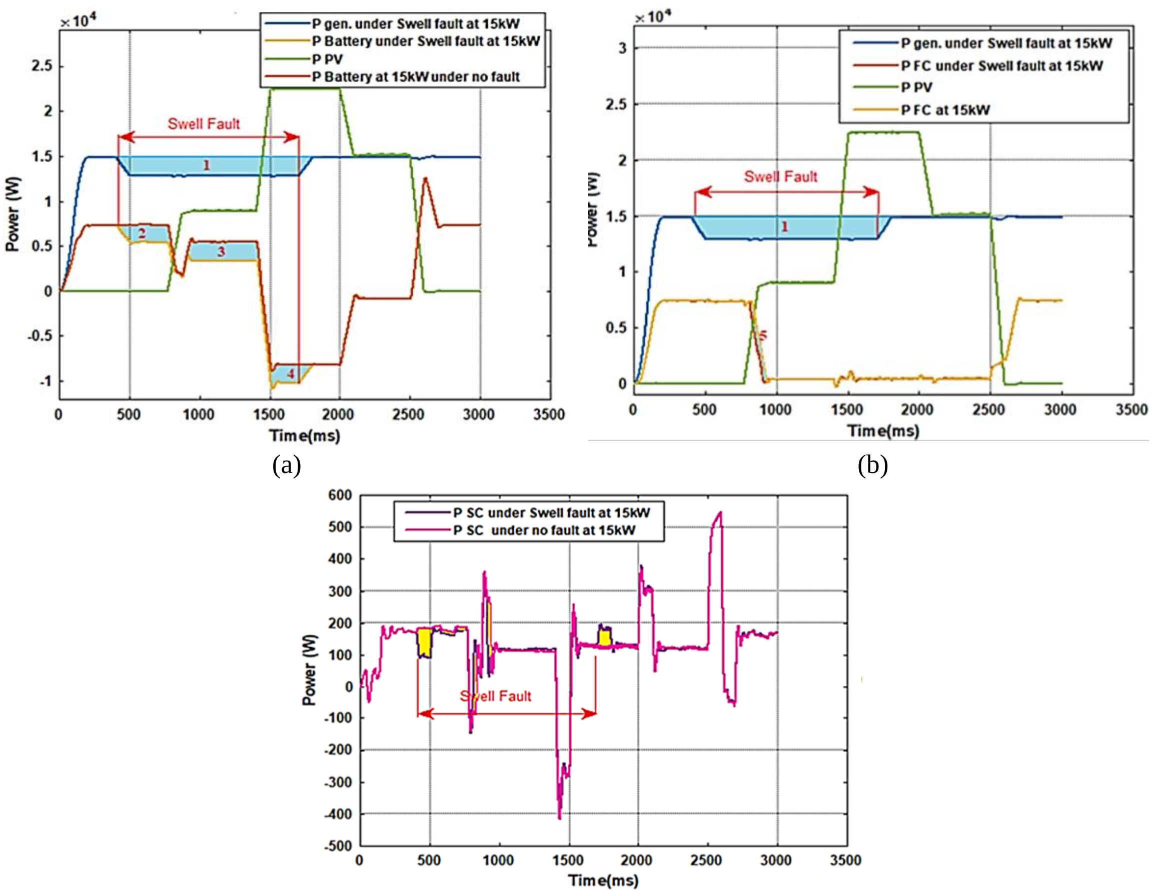

Figure 8. Contribution of Battery, FC and SC during swell disturbance: (a) battery power, (b) FC power, and (c) SC power

Figure 9 presents the DC bus voltage (V_{DC}) profile under both voltage sag and swell disturbances, compared with the nominal 500 V under no-fault conditions. During the test, a small positive deviation of +0.7 V occurs at t = 0.7 s, followed by a maximum positive peak of +1.4 V at t = 1.4 s. The maximum negative deviation reaches –2.7 V at t = 2.571 s, reducing V_{DC} to 497.3 V. These limited DC-link voltage fluctuations, confined to within ±0.54%, remain well inside acceptable operational margins and are primarily induced by PV irradiance variations, thereby confirming the effectiveness of the proposed control strategy in maintaining DC-link voltage regulation and ensuring robust system operation under dynamic conditions.

Figure 10 shows the battery current and SoC under voltage sag and swell at 15 bkW. The battery alternates between discharging and charging to compensate for deficits and absorb excess PV energy (Figure 10(a)), with SoC decreasing during discharge and rising during charge (Figure 10(b)), demonstrating dynamic coordination under transient conditions compared to normal operation.

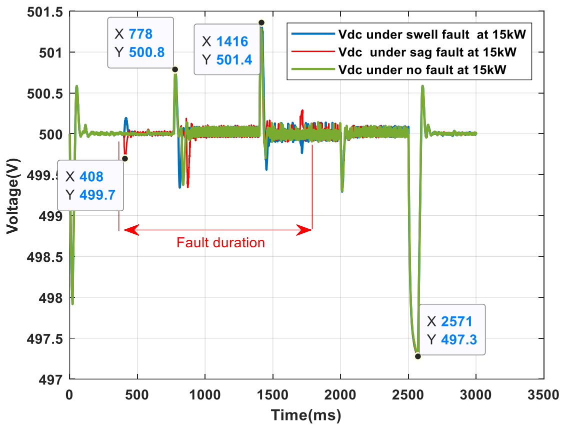

Figure 9. VDC bus under sag and swell compared to VDC under normal conditions at 15 kW load

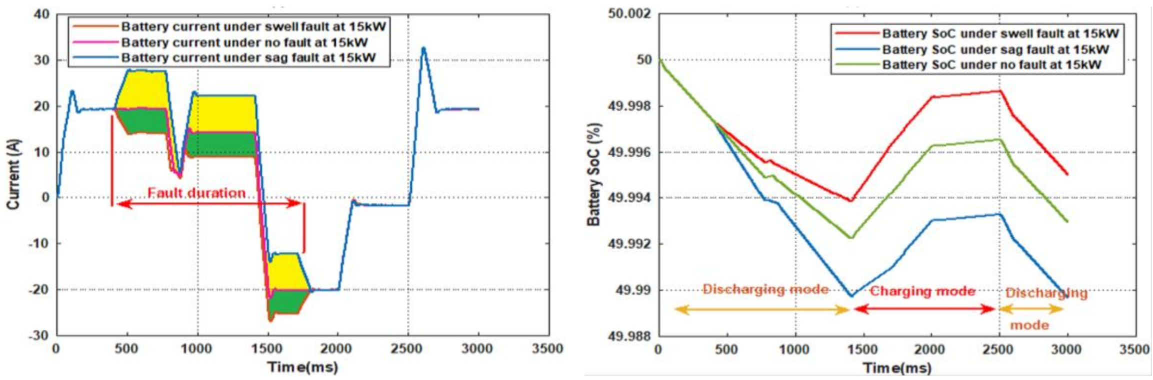

(a) (b)

Figure 10. Battery current and SoC under voltage sag and swell disturbances, compared with battery current during normal operation at a 15-kW load: (a) battery current and (b) battery SoC

3.4. Comparative analysis, scalability, and practical considerations

Table 2 compares the proposed EMS–DVR framework with representative hybrid energy management and power-quality enhancement approaches reported in recent literature. The comparison considers DVR integration, hybrid storage configuration, EMS methodology, DC-bus stability, and battery stress mitigation capability to evaluate the relative advantages of the proposed coordinated control strategy. As shown in Table 2, most existing studies investigate either hybrid EMS coordination or power-quality enhancement separately. In contrast, the proposed framework combines real-time fuzzy EMS, battery–supercapacitor–fuel cell coordination, and DVR-assisted voltage compensation within a unified DC microgrid architecture. The proposed coordinated strategy achieves improved DC-bus stability and reduced battery stress under severe voltage disturbances through fast supercapacitor transient compensation and adaptive power sharing among the hybrid sources. Beyond the comparative performance evaluation, the proposed EMS–DVR framework also demonstrates strong potential for practical smart-grid applications.

The modular hybrid storage architecture facilitates scalability toward larger DC microgrids integrating multiple distributed energy resources (DERs), EV charging stations, and critical loads requiring high reliability and power quality. Furthermore, coordinated supercapacitor-based transient compensation can reduce battery cycling stress and potentially lower long-term maintenance and replacement costs. The computational simplicity of the fuzzy controller also makes the proposed approach suitable for embedded and real-time digital implementation in future intelligent microgrid systems.

Nevertheless, practical deployment of the proposed framework introduces several challenges, including increased converter count, communication and coordination requirements, accurate real-time SoC estimation, and validation under hardware operating conditions. In addition, long-term storage degradation and harmonic compensation performance were not explicitly investigated in the present study and remain important directions for future research.

Table 2. Comparative analysis of the proposed EMS-DVR framework with recent studies

Reference	DVR integration	Hybrid storage configuration	EMS technique	Main focus	DC-bus stability	Battery stress reduction
Albasheri *et al.* [8]	No	Battery + SC	Hybrid EMS	DC microgrid energy management	Moderate	Moderate
Wang [10]	No	Battery + SC	Compensation-based control	Hybrid storage compensation topology	Good	Moderate
Al-Salloomee *et al.* [11]	No	Battery + SC	Conventional power management	Standalone DC microgrid operation	Moderate	Limited
Smith *et al.* [12]	No	Battery-based ESS	Fuzzy EMS	Fuzzy control in DC microgrids	Good	Moderate
Elmetwaly *et al.* [26]	No dedicated DVR	Hybrid ESS	EMS + power quality control	Microgrid operation and PQ enhancement	Good	Moderate
Proposed method	Yes	Battery + SC + FC	Real-time fuzzy EMS	Integrated EMS and DVR-assisted PQ enhancement	±1.18% at 500 V under 0.2 pu sag/ 1.6 pu swell	High through SC transient compensation

4. CONCLUSION

This paper proposed a real-time fuzzy-based coordination framework for hybrid energy storage systems (HESS) in a DVR-assisted DC microgrid, integrating DC-side energy management and AC-side power quality enhancement within a unified control architecture. The proposed strategy combines a priority-based EMS (PV → SC → battery → FC) with dynamic voltage restorer operation to ensure coordinated energy sharing and voltage disturbance mitigation under dynamic operating conditions.

Simulation results under severe voltage disturbances, including 0.2 pu sag and 1.6 pu swell conditions, demonstrated effective coordination among the supercapacitor, battery, and fuel cell according to their dynamic characteristics. The supercapacitor provided rapid transient compensation, the battery ensured intermediate energy support, and the fuel cell supplied long-term power balancing. Consequently, the proposed framework maintained the DC bus voltage within ±1.18% of the nominal 500 V value while enhancing power quality and system stability. Beyond simulation performance, the proposed framework shows strong potential for practical renewable-energy integration in advanced DC microgrids requiring reliable operation, disturbance tolerance, and intelligent energy coordination. By improving DC-link stability and reducing stress on storage devices and power electronic converters, the proposed EMS–DVR strategy can contribute to enhanced inverter reliability, improved power quality, and increased smart-grid resilience under fluctuating renewable generation and load conditions. Furthermore, the computational simplicity of the fuzzy controller makes the proposed approach suitable for real-time implementation in future intelligent microgrid applications. Future work will include hardware-in-the-loop and experimental validation, alongside AI-assisted EMS strategies for resilient, self-healing smart microgrids.

FUNDING INFORMATION

Authors state no funding involved.

AUTHOR CONTRIBUTIONS STATEMENT

This journal uses the Contributor Roles Taxonomy (CRediT) to recognize individual author contributions, reduce authorship disputes, and facilitate collaboration.

Name of Author	C	M	So	Va	Fo	I	R	D	O	E	Vi	Su	P	Fu
Yacine Benatallah		✓	✓	✓	✓			✓	✓	✓			✓	
Abdelkrim Benali	✓	✓	✓			✓		✓	✓	✓		✓		
Mabrouk Dahane	✓			✓			✓			✓	✓			
Somia Benali	✓	✓							✓	✓			✓	

C : **C**onceptualization
M : **M**ethodology
So : **So**ftware
Va : **Va**lidation
Fo : **Fo**rmal analysis
I : **I**nvestigation
R : **R**esources
D : **D**ata Curation
O : Writing - **O**riginal Draft
E : Writing - Review & **E**diting
Vi : **Vi**sualization
Su : **Su**pervision
P : **P**roject administration
Fu : **Fu**nding acquisition

CONFLICT OF INTEREST STATEMENT

Authors state no conflict of interest.

DATA AVAILABILITY

Data availability is not applicable to this paper as no new data were created or analyzed in this study.

REFERENCES

[1] M. K. Khan, M. Raza, M. Shahbaz, U. Farooq, and M. U. Akram, "Recent advancement in energy storage technologies and their applications," *Journal of Energy Storage*, vol. 92, Art. no. 112112, 2024, doi: 10.1016/j.est.2024.112112.

[2] R. J. Kumar, P. Vijayakumar, S. Paramasivam, A. Kumar, and G. Gatto, "Hybrid WbOA–APINN framework for sustainable and intelligent energy management in renewable microgrids with hybrid energy storage," *Electric Power Systems Research*, vol. 252, p. 112349, 2026, doi: 10.1016/j.epsr.2025.112349.

[3] S. Gupta, Y. Sawle, K. Thakre, and M. Thirunavukkarasu, "Techno-economic-environmental analysis of hybrid renewable energy system with lead acid and lithium-ion energy storage under different PV tracking orientations," *Journal of Energy Storage*, vol. 130, p. 117417, 2025, doi: 10.1016/j.est.2025.117417.

[4] E. Villa-Avila, D. Ochoa-Correa, P. Arévalo-Cordero, F. Jurado, and L. Sigüenza-Guzmán, "Real-time photovoltaic smoothing with supercapacitors: Low-complexity supervisory selection of conventional filters," *Electric Power Systems Research*, vol. 254, p. 112696, 2026, doi: 10.1016/j.epsr.2025.112696.

[5] A. M. Adeyinka, O. C. Esan, A. O. Ijaola *et al.*, "Advancements in hybrid energy storage systems for enhancing renewable energy-to-grid integration," *Sustainable Energy Research*, vol. 11, art. no. 26, 2024, doi: 10.1186/s40807-024-00120-4.

[6] T. H. B. Huy, T.-D. Le, P. V. Phu, S. Park, and D. Kim, "Real-time power scheduling for an isolated microgrid with renewable energy and energy storage system via a supervised-learning-based strategy," *Journal of Energy Storage*, vol. 88, p. 111506, 2024, doi: 10.1016/j.est.2024.111506.

[7] N. Mbuli, "Dynamic voltage restorer as a solution to voltage problems in power systems: Focus on sags, swells and steady fluctuations," *Energies*, vol. 16, no. 19, art. no. 6946, 2023, doi: 10.3390/en16196946.

[8] M. A. Albasheri, O. Bouchhida, Y. Soufi, A. Cherifi, and M. A. H. Mujammal, "Energy management technique of hybrid energy storage system-based DC microgrid," *Journal of Energy Systems*, vol. 9, no. 1, pp. 36–51, Mar. 2025.

[9] M. A. Albasheri, O. Bouchhida, Y. Soufi, and A. Cherifi, "Enhanced energy storage system efficiency for remote area-based DC microgrid," *Studies in Engineering and Exact Sciences*, vol. 5, no. 2, 2024, doi: doi.org/10.54021/seesv5n2-002.

[10] L. Wang, "Oilfield microgrid-oriented supercapacitor-battery hybrid energy storage system with series-parallel compensation topology," *Processes*, vol. 13, no. 6, 2025, doi: 10.3390/pr13061689.

[11] S. Al-Salloomee *et al*., "Study of power management of standalone DC microgrids with battery-supercapacitor hybrid energy storage system," *International Journal of Electrical and Computer Engineering (IJECE)*, vol. 12, no. 1, 2022, doi. 10.11591/ijece.v12i1.pp114-121.

[12] R. D. Smith *et al.*, "Fuzzy control of energy storage systems in DC microgrids," *Proceedings of COMPEL*, 2019, pp. 1–8, doi: 10.1109/COMPEL.2019.8769610.

[13] V. Subramanian *et al.*, "Cognitive fuzzy logic-integrated energy management for microgrids," *Energies*, vol. 18, no. 1, Art. no 122, 2025.

[14] M. Alshareef, Z. Lin, M. Ma, and W. Cao, "Accelerated particle swarm optimization for photovoltaic maximum power point tracking under partial shading conditions," *Energies*, vol. 12, no. 4, p. 623, Feb. 2019, doi: 10.3390/en12040623.

[15] M. S. Endiz, G. Gökkuş, A. E. Coşgun, and H. Demir, "A review of traditional and advanced MPPT approaches for PV systems under uniform insolation and partially shaded conditions," *Applied Sciences*, vol. 15, no. 3, Art. no. 1031, 2025.

[16] A. Benali, M. Khiat, T. Allaoui, and M. Denaï, "Power quality improvement and low voltage ride through capability in hybrid wind-PV farms grid-connected using dynamic voltage restorer," *IEEE Access*, vol. 6, pp. 68634–68648, 2018, doi: 10.1109/ACCESS.2018.2878493.

[17] B. Xia, P. Guo, X. Wei, and H. Zong, "Reaction gas pressure, temperature, and membrane water content modulate electrochemical process of a PEMFC: A simulation study," *Advances in Materials Science and Engineering*, 2023.

[18] S. Atyabi, E. Afshari, and N. Shakarami, "Three-dimensional multiphase modeling of the performance of an open-cathode PEM fuel cell with additional cooling channels," *Energy*, vol. 263, 2023, Art. no. 0360544222023891.

[19] T. Teng, X. Zhang, Q. Xue, and B. Zhang, "Research of proton exchange membrane fuel cell modeling on concentration polarization under variable-temperature operating conditions," *Energies*, vol. 17, no. 3, Art. no. 730, 2024, doi: 10.3390/en17030730

[20] M. Chen and G. A. Rincon-Mora, "Accurate electrical battery model capable of predicting runtime and IV performance*," IEEE Trans. Energy Convers*., vol. 21, no. 2, pp. 504–511, 2006.

[21] P. Simon and Y. Gogotsi, "Materials for electrochemical capacitors," *Nature Materials*, vol. 7, no. 11, pp. 845–854, 2008.

[22] L. Zhang, "A review of supercapacitor modeling, estimation, and applications: a control/management perspective," *Renewable and Sustainable Energy Reviews*, vol. 81, pp. 1868–1878, 2018, doi: 10.1016/j.rser.2017.05.283.
[23] M. E. Sahin, F. Blaabjerg, and A. Sangwongwanich, "Modelling of supercapacitors based on simplified equivalent circuit," *CPSS Transactions on Power Electronics and Applications*, vol. 6, no. 1, pp. 31–39, 2021, doi: 10.24295/CPSSTPEA.2021.00003.
[24] F. Naseri *et al.*, "Supercapacitor management system: A comprehensive review," *Renewable and Sustainable Energy Reviews*, vol. 155, 2022, doi: 10.1016/j.rser.2021.111913.
[25] A. Moghassemi and S. Padmanaban, "Dynamic voltage restorer (DVR): A comprehensive review of topologies, power converters, control methods, and modified configurations," *Energies*, vol. 13, no. 16, p. 4152, 2020, doi: 10.3390/en13164152.
[26] A. H. Elmetwaly, A. A. ElDesouky, A. I. Omar, and M. A. Saad, "Operation control, energy management, and power quality enhancement for a cluster of isolated microgrids," *Ain Shams Engineering Journal*, vol. 13, no. 5, Art. no. 101737, 2022, doi: 10.1016/j.asej.2022.101737.
[27] W. Huang, "Hierarchical coordinated energy management strategy for hybrid energy storage system in electric vehicles considering the battery's SOC," *Systems*, vol. 11, no. 10, Art. no. 498, 2023, doi: /10.3390/systems11100498

BIOGRAPHIES OF AUTHORS

Yacine Benatallah is a Ph.D. student in electrical engineering at Nour Bachir University Center in El Bayadh, Algeria. He received his Master's degree in electrical engineering, specializing in industrial electrotechnics, from Amar Thelidji University of Laghouat in 2021. His research focuses on the modeling, control, and supervision of remote energy plant systems. He is currently a member of the Instrumentation Laboratory and Advanced Materials at Nour El Bachir University Center, El Bayadh, Algeria. He can be contacted at email: yacinee.benatallah@gmail.com.

Abdelkrim Benali is an academic and electrical engineer with extensive experience in industry and higher education. He received his Engineer degree in electrotechnics from Saida University in 1998, followed by a Master's degree in 2011 and a Ph.D. in electrical engineering from the National Polytechnic School of Oran, specializing in advanced electrical systems and embedded electronics for renewable energy. He began his career with practical experience in electrical control, installation, and maintenance before transitioning to academia in 2012. He currently serves as a lecturer in the Department of Electrical Engineering at Nour Bachir University Center of El-Bayadh, Algeria. His teaching portfolio includes undergraduate and graduate courses such as electrical devices, control systems, programmable logic controllers (PLCs), and microcontrollers. His research interests include remote laboratories, embedded electronics for renewable energy systems, and artificial intelligence. He can be contacted at email: benaliabd@gmail.com.

Mabrouk Dahane received his B.Sc. degree in electrical engineering from Tahri Mohammed University of Bechar, Algeria, in 2020, and his M.Sc. degree in control of electrical systems from Tahri Mohammed University of Bechar, Algeria, in 2022. He is currently a Ph.D. student and a member of the Instrumentation Laboratory and Advanced Materials at Nour El Bachir University Center, El Bayadh, Algeria. His research interests include supervision and control of wind energy systems, power control, robust control, and optimization methods. He can be contacted at email: m.dahane@cu-elbayadh.dz.

Somia Benali earned her Ph.D. in Management Sciences from the University of Relizane. Her areas of expertise include information and communication technologies (ICT), innovation, and e-commerce. Her research focuses on technological, marketing, and operational innovation in the context of digital transformation, with particular emphasis on the development of e-commerce in Algeria, its challenges, growth opportunities, and impact on the national economy. She is also interested in the application of artificial intelligence in e-commerce, including recommendation systems, customer service automation, predictive analytics, and intelligent customer data management. In addition to her academic expertise, she has strong skills in web development, enabling her to design, analyze, and implement digital platforms tailored to the evolving needs of online commerce. Her combination of theoretical knowledge and technical expertise enables her to contribute effectively to the digitalization and innovation of businesses in Algeria. She can be contacted at email: benalisomia1710@gmail.com.